

Temperature dependence of side-jump spin Hall conductivity

Cong Xiao^{1,*}, Yi Liu², Zhe Yuan^{2,†}, Shengyuan A. Yang³, and Qian Niu¹

¹*Department of Physics, The University of Texas at Austin, Austin, Texas 78712, USA*

²*The Center for Advanced Quantum Studies and Department of Physics, Beijing Normal University, 100875 Beijing, China and*

³*Research Laboratory for Quantum Materials, Singapore University of Technology and Design, Singapore 487372, Singapore*

In the conventional paradigm of the spin Hall effect, the side-jump contribution to the spin Hall conductivity is independent of the density of disorder, thus remains unchanged in clean samples when the phonon density varies with temperature. To the contrary, we show a temperature-dependent side-jump contribution due to electron-phonon scattering at low temperature when the equipartition law breaks down. The physical mechanism resulting in this temperature dependence differs from that of the phonon-induced longitudinal resistivity. We demonstrate this phenomenon in an analytic model, supplemented by a first-principles calculation for pure Pt. Experimentally accessible high-purity Pt is proposed to be suitable for observing the predicted prominent variation of the spin Hall conductivity below 80 K.

The spin Hall effect refers to a transverse spin current in response to an external electric field [1]. In strongly spin-orbit-coupled electronic systems such as $4d$ and $5d$ transition metals [2–10] and Weyl semimetals [11], the disorder-independent spin Hall contribution due solely to the geometry of Bloch bands, the so-called spin Berry curvature, has attracted much attention. Besides, there is a scattering induced mechanism called side-jump, whose contribution to the spin Hall conductivity (SHC) turns out to be independent of the density of a given type of impurities [1]. Furthermore, the side-jump SHC is also regarded as remaining unchanged when the phonon density varies with temperature (T) [12, 13]. Therefore, it has been a great challenge to separate the geometric and the side-jump contributions in a metallic material.

In this letter we demonstrate that the side-jump SHC arising solely from the electron-phonon (el-ph) scattering is T -dependent at the temperature below the classical equipartition regime where the longitudinal resistivity ρ is linear in T . This character of side-jump distinguishes itself from the geometric contribution, and provides a new mechanism for T -dependent SHCs in high-purity experimental samples.

The side-jump was originally proposed as the side-way shift in opposite transverse directions for the carriers with different spins, when they are scattered by spin-orbit active impurities [12, 14]. This picture works well in the systems with weak spin-orbit interaction [15–17], where the spin-orbit-induced band splitting is smeared by the disorder broadening [1]. Whereas in strongly spin-orbit-coupled Bloch bands of current interest, the side-jump contribution arises microscopically from the scattering-induced interband elements of the out-of-equilibrium density matrix [18–21]. This corresponds to in the phenomenological Boltzmann transport formalism the dressing of Bloch states by interband virtual scattering processes involving off-shell states (away from the Fermi surface) [22]. This effect modifies the semiclassical velocity of carriers by a so-called “side-jump

velocity” [19–23] which is related to the coordinate-shift of carriers during scattering off scalar disorder [20]. The transverse component of the side-jump velocity is just the extension of the original side jump [12, 14]. When the transported spin component is not a good quantum number, the scattering-induced dressing of carrier states provides the counterpart of the side-jump velocity for spin current [22, 24].

We consider a non-degenerate multiband system with strong spin-orbit coupling in the weak scattering regime. The quasi-static treatment for phonons is used to provide semi-quantitative and intuitive understanding. In this treatment the quantum dynamics of phonons are neglected, and the el-ph scattering is approximated by a single-electron elastic scattering with quasi-static scatterers obeying bosonic statistics. Therefore, the Boltzmann transport theory formulated for weak static scatterers [18, 22, 23] with some input concerning the el-ph interaction can be employed to proceed. In the calculation of the resistivity resulting from phonon scattering, the quasi-static approximation produces not only the correct low- T power law ($\rho \sim T^5$ for 3D isotropic single-Fermi-surface systems) [25] but also the values that are quantitatively comparable with experimental data [26].

Transport formalism involving off-shell states.—In weakly disordered crystals perturbed by an weak external electric field \mathbf{E} , the expectation value of an observable \mathbf{A} (assumed to be a vector without loss of generality) reads

$$\langle \mathbf{A} \rangle = \sum_l \mathbf{A}_l f_l \quad (1)$$

in the Boltzmann transport formalism, where f_l is the occupation function of the carrier state marked by $l = (\eta, \mathbf{k})$ with η the band index and \mathbf{k} the crystal momentum, \mathbf{A}_l is the quantum mechanical average on state l . The carrier state is the Bloch state dressed by interband virtual processes induced by both the electric field and scattering [22]. In the linear response and weak scattering regime,

these two dressing effects are independent [22]:

$$\mathbf{A}_l = \mathbf{A}_l^0 + \delta^{\text{bc}} \mathbf{A}_l + \delta^{\text{sj}} \mathbf{A}_l, \quad (2)$$

where (e is the carrier charge) $(\delta^{\text{bc}} \mathbf{A}_l)_\beta = \frac{e}{\hbar} \mathbf{E}_\alpha \Omega_{\alpha\beta}^A(\eta\mathbf{k})$ with (spin Berry curvature when \mathbf{A} is the spin current)

$$\Omega_{\alpha\beta}^A(\eta\mathbf{k}) = -2\hbar^2 \text{Im} \sum_{\eta'' \neq \eta} \frac{v_\alpha^{\eta\eta''}(\mathbf{k}) A_\beta^{\eta''\eta}(\mathbf{k})}{(\epsilon_{\eta\mathbf{k}} - \epsilon_{\eta''\mathbf{k}})^2}, \quad (3)$$

and

$$\begin{aligned} (\delta^{\text{sj}} \mathbf{A}_l)_\beta &= -2\pi \sum_{\eta'\mathbf{k}'} W_{\mathbf{k}\mathbf{k}'} \delta(\epsilon_{\eta\mathbf{k}} - \epsilon_{\eta'\mathbf{k}'}) \\ &\times \text{Im} \left[\sum_{\eta'' \neq \eta'} \frac{\langle u_{\eta\mathbf{k}} | u_{\eta'\mathbf{k}'} \rangle \langle u_{\eta''\mathbf{k}'} | u_{\eta\mathbf{k}} \rangle A_\beta^{\eta'\eta''}(\mathbf{k}')}{\epsilon_{\eta'\mathbf{k}'} - \epsilon_{\eta''\mathbf{k}'}} \right. \\ &\left. - \sum_{\eta'' \neq \eta} \frac{\langle u_{\eta''\mathbf{k}} | u_{\eta'\mathbf{k}'} \rangle \langle u_{\eta'\mathbf{k}'} | u_{\eta\mathbf{k}} \rangle A_\beta^{\eta\eta''}(\mathbf{k})}{\epsilon_{\eta\mathbf{k}} - \epsilon_{\eta''\mathbf{k}}} \right]. \quad (4) \end{aligned}$$

Equation (4) is diagrammatically represented in Fig. 1. The summation over repeated spatial indices α, β is implied hereafter. Here $A_\beta^{\eta'\eta}(\mathbf{k}) \equiv \langle u_{\eta'\mathbf{k}} | A_\beta | u_{\eta\mathbf{k}} \rangle$ with $|u_{\eta\mathbf{k}}\rangle$ the periodic amplitude of the Bloch state. For impurities $W_{\mathbf{k}\mathbf{k}'} = n_i |V_{\mathbf{k}\mathbf{k}'}^o|^2$, with n_i the impurity density and $V_{\mathbf{k}\mathbf{k}'}^o$ the plane-wave part of the matrix element of the impurity potential. For quasi-static el-ph scattering

$$W_{\mathbf{k}\mathbf{k}'} = \frac{2N_{\mathbf{q}}}{V} |U_{\mathbf{k}\mathbf{k}'}^o|^2, \quad (5)$$

where $U_{\mathbf{k}'\mathbf{k}}^o$ is the plane-wave part of the el-ph matrix element, $N_{\mathbf{q}}$ is the Bose occupation function of phonons (\mathbf{q} is the wave-vector of phonons with energy $\hbar\omega_{\mathbf{q}}$), V is the volume (area in 2D) of the system, and the factor 2 accounts for the absorption and emission of phonons. Neglecting the quantum dynamics of phonons implies that the quantum zero-point motion is thrown away [25] thus $2(N_{\mathbf{q}} + 1/2) \rightarrow 2N_{\mathbf{q}}$. This treatment is necessary for the correct low- T asymptotic behavior in the quasi-static approximation, as pointed out by Ziman [25].

The carrier occupation function is decomposed, around the Fermi distribution f_l^0 , into $f_l = f_l^0 + g_l^{2s} + g_l^a$, satisfying the linearized steady-state Boltzmann equations $e\mathbf{E} \cdot \mathbf{v}_l^0 \partial f_l^0 / \partial \epsilon_l = -\sum_{l'} w_{ll'}^{2s} (g_l^{2s} - g_{l'}^{2s})$ and $(\partial_{\epsilon_l} \equiv \partial / \partial \epsilon_l)$

$$e\mathbf{E} \cdot \delta^{\text{sj}} \mathbf{v}_l \partial_{\epsilon_l} f_l^0 = \sum_{l'} w_{ll'}^{2s} (g_l^a - g_{l'}^a) \quad (6)$$

in the presence of quasi-static weak scalar disorder [20]. $w_{ll'}^{2s} = \frac{2\pi}{\hbar} W_{\mathbf{k}\mathbf{k}'} |\langle u_l | u_{l'} \rangle|^2 \delta(\epsilon_l - \epsilon_{l'})$ is the lowest-Born-order scattering rate, \mathbf{v}_l^0 is the usual band velocity.

Collecting the above ingredients, the spin Hall current is $j_{\text{SH}} = j_{\text{SH}}^{\text{bc}} + j_{\text{SH}}^{\text{sj}} + j_{\text{SH}}^{\text{ad}}$. The first two terms

$$j_{\text{SH}}^{\text{bc}} = \sum_l (\delta^{\text{bc}} j_l) f_l^0, \text{ and } j_{\text{SH}}^{\text{sj}} = \sum_l (\delta^{\text{sj}} j_l) g_l^{2s} \quad (7)$$

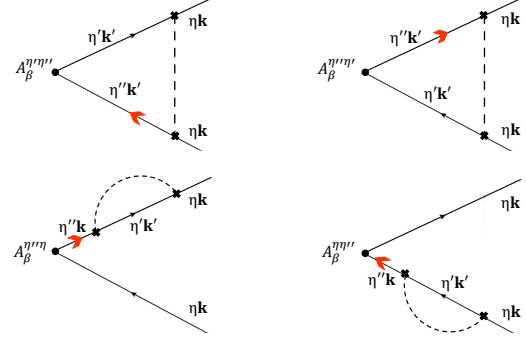


FIG. 1. Graphical representation of Eq. (4), where the off-shell states are marked by red arrows. $W_{\mathbf{k}\mathbf{k}'}$ is represented by the disorder line connected with two interaction vertexes.

arise from off-shell-states induced corrections to the semiclassical value of j_l^0 . Whereas $j_{\text{SH}}^{\text{ad}} = \sum_l j_l^0 g_l^a$ incorporates the nonequilibrium occupation function modified by off-shell states, since g_l^a appears as a response to the generation term proportional to $\delta^{\text{sj}} \mathbf{v}_l$ [23]. Both $j_{\text{SH}}^{\text{sj}}$ and $j_{\text{SH}}^{\text{ad}}$ are the zeroth-order homogeneous terms of $W_{\mathbf{k}\mathbf{k}'}$. In calculating the anomalous Hall (AH) current [19] $\mathbf{A} = e\mathbf{v}$, $j_{\text{AH}}^{\text{sj}}$ and $j_{\text{AH}}^{\text{ad}}$ are related to the transverse (side-way) and longitudinal components of $\delta^{\text{sj}} \mathbf{v}_l$, respectively [23]. Thereby their sum is also often referred to as the side-jump contribution in the literature on the anomalous Hall effect [19, 20, 23]. Given this convention, we also present results for $j_{\text{SH}}^{\text{ad}}$. However, $j_{\text{AH}}^{\text{ad}}$ has nothing to do with the original concept of side-jump, and the microscopic theory [18, 21] indeed shows that g_l^a is not related to the interband elements of the out-of-equilibrium density matrix. In fact, in 2D nonmagnetic models for the spin Hall effect, such as the 2D electronic systems with Rashba, cubic Rashba and Dresselhaus spin-orbit couplings [27–32], the spin current operator (for out-of-plane spin component) has only interband matrix elements, i.e., $j_l^0 = 0$, thus $j_{\text{SH}}^{\text{ad}}$ does not appear at all [33, 34].

Phonon-induced SHC in the low- T and high- T limits.—In order to show the T -dependence of the phonon-induced (without impurities) side-jump SHC, we prove that its values in the low- T and high- T limits can be different. In realistic systems where the inevitable impurity scattering dominates the transport properties in the low- T limit, the phonon-induced behavior shows up at low but finite temperatures and is more remarkable in high-purity samples (detailed later in Fig. 2)).

In the low- T limit, $W_{\mathbf{k}\mathbf{k}'}$ for el-ph scattering is highly peaked at vanishing scattering angle, and the on-shell scattering can only be the intraband transition, hence $\eta' = \eta$ and \mathbf{k}' is very close to \mathbf{k} in Eq. (4). We can then expand the integrand up to the first order of $(\mathbf{k}' - \mathbf{k})$,

getting a compact form of $\delta^{\text{sj}}\mathbf{A}_l$:

$$\left(\delta^{\text{sj}}\mathbf{A}_l\right)_\beta = \sum_{\mathbf{k}'} \tilde{w}_{l'l}^{2s} \Omega_{\alpha\beta}^A(\eta\mathbf{k}) (\mathbf{k}' - \mathbf{k})_\alpha, \quad (8)$$

with $\tilde{w}_{l'l}^{2s} = \frac{2\pi}{\hbar} W_{\mathbf{k}\mathbf{k}'} \delta(\epsilon_{\eta\mathbf{k}} - \epsilon_{\eta\mathbf{k}'})$ the lowest-Born-order scattering rate in the small-scattering-angle limit where $|\langle u_{\eta\mathbf{k}} | u_{\eta\mathbf{k}'} \rangle|^2 \rightarrow 1$. Concurrently, $\delta^{\text{sj}}\mathbf{v}_l = \sum_{\mathbf{k}'} \tilde{w}_{l'l}^{2s} \boldsymbol{\Omega}(l) \times (\mathbf{k}' - \mathbf{k})$ ($\boldsymbol{\Omega}$ is the vector form of the Berry curvature) yields $g_l^\alpha = e\mathbf{E} \cdot [\mathbf{k} \times \boldsymbol{\Omega}(l)] \partial_{\epsilon_l} f_l^0$. Thus one has [34]

$$\left(j_{\text{SH}}^{\text{sj}}\right)_\beta = e \sum_l \mathbf{k}_\alpha \Omega_{\alpha\beta}^j(l) \mathbf{E} \cdot \mathbf{v}_l^0 \partial_{\epsilon_l} f_l^0, \quad (9)$$

and $(j_{\text{SH}}^{\text{ad}})_\beta = e \sum_l (j_l^0)_\beta \mathbf{E} \cdot [\mathbf{k} \times \boldsymbol{\Omega}(l)] \partial_{\epsilon_l} f_l^0$. In the low- T limit, $\sigma_{\text{SH}} = (j_{\text{SH}})_x / E_y$ is a T -independent constant. It is clear that this constant equals to that contributed by scalar-impurities in the long-range limit.

In the high- T limit, the phonon energy is much smaller than $k_B T$ indicating $W_{\mathbf{k}\mathbf{k}'} = 2k_B T V^{-1} |U_{\mathbf{k}'\mathbf{k}}^o|^2 / \hbar\omega_q$, then we have $g_l^{2s} \sim T^{-1}$, $\delta^{\text{sj}}j_l \sim T$, and $g_l^a \sim T^0$, and consequently,

$$\rho \sim T, \quad \sigma_{\text{SH}} \sim T^0. \quad (10)$$

It is apparent that this T -independent σ_{SH} can be different from that in the low- T limit.

To acquire a more intuitive and transparent picture, we consider a dilute metallic system with low carrier density compared to common 3D metals [35–37]. Then its Fermi surface is much smaller than the phonon Debye-sphere and does not support el-ph Umklapp processes, so any large-angle el-ph scattering can occur via normal processes. We also take the approximation of el-ph coupling constant [38] $\lambda^2 = 2V^{-1} |U_{\mathbf{k}'\mathbf{k}}^o|^2 / \hbar\omega_q$, i.e., the deformation-potential electron-acoustic phonon coupling, hence we arrive at $W_{\mathbf{k}\mathbf{k}'} = \lambda^2 k_B T$ in the high- T regime. Thus we can obtain $g_l^{2s,ep} \lambda^2 k_B T = g_l^{2s,ei} n_i V_i^2$, $(\delta^{\text{sj}}\mathbf{A}_l)^{ep} / \lambda^2 k_B T = (\delta^{\text{sj}}\mathbf{A}_l)^{ei} / n_i V_i^2$ and $g_l^{a,ep} = g_l^{a,ei}$, where the superscript "ep" and "ei" mean the contributions due to el-ph scattering and zero-range scalar impurities, respectively. In the latter case, we have $W_{\mathbf{k}\mathbf{k}'} = n_i V_i^2$ with V_i the strength of impurities. Thereby σ_{SH} due to phonons in the high- T regime takes the same value as that due to zero-range scalar impurities.

Phonon-induced T -dependence of SHC.—In the conventional paradigm of the spin Hall effect the side-jump SHC remains unchanged as the density of a given type of scatterers varies. This is no longer the case for phonons. According to the above results, in a dilute metal σ_{SH} induced by electron-acoustic phonon scattering is T -dependent provided that the σ_{SH} induced by scalar impurity scattering in the long-range and zero-range limits are different. Note that the mechanism resulting in this T -dependence differs from that for the T -dependent ρ , because the side-jump SHC and ρ have different scaling

with the scattering time or W (order of W^0 and of W^1 , respectively). To directly see this point, one need just consider the fact that at high temperatures $\sigma_{\text{SH}} \sim T^0$ but $\rho \sim T$.

To be precise, we discuss some model systems, which have the T -independent or T -dependent SHCs depending on its specific Hamiltonian. In the 2D electron gas with k -linear Rashba spin-orbit coupling, the side-jump SHC induced by scalar disorder always cancels the spin Berry curvature contribution as a result of the covariant conservation law for the spin current [27]. Thus the side-jump SHC from scalar impurities does not depend on the scattering range, and that from el-ph scattering does not depend on temperature in this model.

On the other hand, there are models characterizing dilute metallic systems which possess different σ_{SH} in the presence of scalar impurities in the long-range and zero-range limits, such as the Luttinger model describing p -type semiconductor [39] and the k -cubic Rashba model for the 2D heavy-hole gas in confined quantum wells [28]. In the latter model [31, 32], the Hamiltonian reads

$$\hat{H} = \frac{\hbar^2 \mathbf{k}^2}{2m} + i \frac{\alpha_R}{2} (\hat{\sigma}_+ k_-^3 - \hat{\sigma}_- k_+^3), \quad (11)$$

where $\mathbf{k} = k(\cos\phi, \sin\phi)$ is the 2D wave-vector, $k_\pm = k_x \pm ik_y$, $\hat{\sigma}_\pm$ are Pauli matrices with $\hat{\sigma}_\pm = \hat{\sigma}_x \pm i\hat{\sigma}_y$, α_R is the spin-orbit coupling coefficient that can be tuned to very large values by the gate voltage [32]. The spin current operator [29, 30] $\hat{j}_x = \frac{3\hbar}{2} \{\hat{\sigma}_z, \hat{v}_x\}$ has only interband components, hence $j_{\text{SH}} = j_{\text{SH}}^{\text{bc}} + j_{\text{SH}}^{\text{sj}}$. The spinor eigenstates read $|u_{\eta\mathbf{k}}\rangle = [1, -i\eta \exp(i3\phi)]^T / \sqrt{2}$, where $\eta = \pm$ labels the two Rashba bands, and the spin Berry curvature is $\Omega_{yx}^j(\eta\mathbf{k}) = -\eta \frac{9\hbar^3 \sin^2\phi}{4m\alpha_R k^3}$, thus $\sigma_{\text{SH}}^{\text{bc}} = (j_{\text{SH}}^{\text{bc}})_x / E_y = \frac{9e\hbar^2}{16\pi m\alpha_R} \sum_\eta \eta k_\eta^{-1}$ [28, 29], with k_η the Fermi wave-number of band η . The side-jump SHC due to phonons in the low- T limit is given by Eq. (9) as

$$\sigma_{\text{SH}}^{\text{sj}} = \left(j_{\text{SH}}^{\text{sj}}\right)_x / E_y = \frac{9e\hbar^2}{64\pi m\alpha_R} \sum_\eta \frac{\eta}{k_\eta} = \frac{1}{4} \sigma_{\text{SH}}^{\text{bc}}. \quad (12a)$$

When $m\alpha_R/\hbar^2 \ll 1/\sqrt{\pi n}$ [29], one has $\sigma_{\text{SH}}^{\text{sj}} = 9e/32\pi$. In the high- T regime, $\delta^{\text{sj}}j_l = 0$ leads to [30]

$$\sigma_{\text{SH}}^{\text{sj}} = 0. \quad (12b)$$

Since the SHCs in the high- T and low- T limits are different, there must be a crossover in the intermediate regime resulting in the T -dependent behavior. We just show schematically the T -dependence of $\sigma_{\text{SH}}^{\text{sj}}$ in this model in Fig. 2, since the concrete calculations are not necessary for our purpose.

One may wonder if the finite phonon-induced $\sigma_{\text{SH}}^{\text{sj}}$ in the low- T limit contradicts to the vanishing phonon density. $\sigma_{\text{SH}}^{\text{sj}}$ can be represented as a function of n_i and T , which has a singularity at the point $n_i = 0$ and $T = 0$

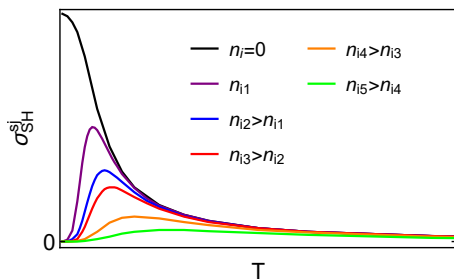


FIG. 2. Schematic illustration of the T -dependence of $\sigma_{\text{SH}}^{\text{sj}}$ in the 2D k -cubic Rashba model in the presence of acoustic phonons and zero-range scalar impurities. The $n_i = 0$ curve is the contribution by phonons alone. Other curves incorporate finite impurity densities $n_{i1} < n_{i2} < n_{i3} < n_{i4} < n_{i5}$.

(see Fig. 2). In realistic systems it is the impurity scattering that determines $\sigma_{\text{SH}}^{\text{sj}}$ in the low- T limit, because in this case $W_{\mathbf{k}'\mathbf{k}} = n_i V_i^2 + \lambda^2 N_q \hbar \omega_q$ is dominated by the impurity term (we assume zero-range scalar impurities), while the phonon term goes to zero. Thereby, in realistic systems the low- T -limit value of $\sigma_{\text{SH}}^{\text{sj}}$ is given by $\lim_{T \rightarrow 0} \sigma_{\text{SH}}^{\text{sj}}(n_i, T)$, which differs from the phonon-induced one acquired by assuming no impurity at first, i.e., $\lim_{T \rightarrow 0} \lim_{n_i \rightarrow 0} \sigma_{\text{SH}}^{\text{sj}}(n_i, T)$. In the presence of finite n_i , at high temperatures $\sigma_{\text{SH}}^{\text{sj}}$ is still the same as that contributed by the zero-range scalar impurities, since $W = n_i V_i^2 + \lambda^2 k_B T$ is k -independent and drops out in the expression for $\sigma_{\text{SH}}^{\text{sj}}$. As temperature decreases, $\sigma_{\text{SH}}^{\text{sj}}$ first changes with temperature according to our previous discussions, but finally evolves to the low- T -limit value dictated by zero-range scalar impurities, which coincides with the high- T one, implying non-monotonic T -dependence (Fig. 2).

Temperature-dependent SHC in pure Platinum.—First we discuss the T -dependent SHCs in 3D metals with large carrier densities, for which the radius of the Debye sphere is smaller than the diameter of the Fermi sphere and thus large-angle el-ph scattering occurs only via Umklapp processes [25]. In the high- T equipartition regime one still has $\rho \sim T$ and $\sigma_{\text{SH}} \sim T^0$, albeit the latter can be different, owing to the Umklapp process, from the σ_{SH} contributed by zero-range scalar impurities. The linear-in- T scaling of ρ usually extends to about $T = T_D/3$ in common metals (e.g., Pt, Cu and Au [26, 40]) with T_D the Debye temperature. At $T < T_D/3$, the equipartition law breaks down and the bosonic occupation of phonons plays an important role, hence ρ departs from the linear- T scaling and σ_{SH} may vary with temperature.

To show the applicability of our theoretical ideas in real materials, we perform a first-principles calculation to the SHC of pure Pt in the range 20 – 300 K. The minimal interband splitting around the Fermi level of Pt is much larger than 300 K [9], thus the spin Berry-curvature contribution should be T -independent up to

300 K. The temperature is modeled by populating the calculated phonon spectra of Pt into a large supercell with its length L along fcc [111] and 5×5 unit cells in the lateral dimensions [26, 41]. Then the transport calculation is carried out using the above disordered (finite-temperature) supercell sandwiched by two perfectly crystalline (zero-temperature) Pt electrodes. The scattering matrix is obtained using the so-called “wave function matching” technique within the Landauer-Büttiker formalism [41]. The calculated total resistance of the scattering geometry is found to be linearly dependent on L following the Ohm’s law. By varying L in the range of 5 – 60 nm, we extract the resistivity at every temperature using a linear least squares fitting for the calculated resistances. For each L , at least 10 random configurations have been considered to ensure both average value and standard deviation well converged with respect to the number of configurations. The calculated resistivity ρ is plotted in Fig. 3(a) as a function of temperature. The spin-Hall angle Θ_{SH} is computed by examining the ratio of transverse spin current density and longitudinal charge current density [10]. At every temperature, we use more than 20 random configurations, each of which contains 60 nm-long disordered Pt. Then the SHC is obtained as $\sigma_{\text{SH}} = (\hbar/e)\Theta_{\text{SH}}/\rho$, shown in Fig. 3(b).

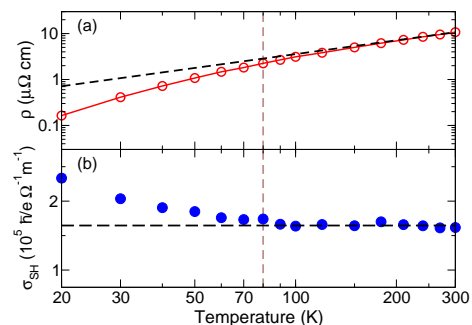


FIG. 3. Calculated longitudinal resistivity ρ (a) and spin Hall conductivity σ_{SH} (b) of pure Pt as a function of temperature. The black dashed line in panel (a) illustrates the linear dependence.

For $T \gtrsim 80$ K, a linear-in- T ρ is obtained, and σ_{SH} is approximately a constant of $1.6 \times 10^5 \hbar/e (\Omega \text{ m})^{-1}$ [10]. Below the equipartition regime, ρ deviates from the linear T -dependence [illustrated by the black dashed line in Fig. 3(a)], concurrently the calculated σ_{SH} increases with decreasing temperature. At $T = 20$ K, σ_{SH} reaches $2.3 \times 10^5 \hbar/e (\Omega \text{ m})^{-1}$. This T -dependence just begins when the temperature drops below the equipartition regime, in agreement with our theoretical prediction.

Finally, we discuss the possibility of observing the predicted effect in experiments. In high-purity metals, the electron-electron scattering dominates over the el-ph scattering in determining transport behaviors at very low temperature. To observe our prediction, lower charac-

teristic temperature T_t marking the crossover from the electron-electron dominated regime to the el-ph dominated one is required, such that the intermediate range from T_t to the high- T equipartition regime is wide enough. In experimentally accessible high-purity Pt samples with residual resistivity as small as $10^{-3} - 10^{-2} \mu\Omega$ cm [42, 43], T_t can be as low as 10K, and at $T = 20$ K the phonon-induced ρ is nearly one order of magnitude larger than that contributed by the electron-electron scattering and the residual resistivity [43]. Because in high-purity Pt, the T -linear scaling of ρ emerges at $T \gtrsim 80$ K [26], the suitable range for observing the first-principles predicted T -dependence of σ_{SH} [Fig. 3(b)] is $20 \text{ K} \lesssim T \lesssim 80$ K. Very recently experimentalists have been developing new techniques, with which the spin current is generated and detected in a single transition-metal sample, thus avoiding all the complications associated with the interfaces and shunting effect [7, 8]. The predicted effect is expected to be observed as the quality of Pt samples in such measurements is improved.

We thank Ming Xie, Tianlei Chai and Haodi Liu for helpful discussions. Q.N. is supported by DOE (DE-FG03-02ER45958, Division of Materials Science and Engineering) on the transport formulation in this work. C.X. is supported by NSF (EFMA-1641101) and Welch Foundation (F-1255). S.A.Y. is supported by Singapore Ministry of Education AcRF Tier 2 (MOE2017-T2-2-108). Y.L. and Z.Y. are supported by the National Natural Science Foundation of China (Grants No. 61604013, No. 61774018, and No. 11734004), the Recruitment Program of Global Youth Experts, and the Fundamental Research Funds for the Central Universities (Grants No. 2016NT10 and No. 2018EYT03).

* congxiao@utexas.edu

† zyuan@bnu.edu.cn

- [1] J. Sinova, S. O. Valenzuela, J. Wunderlich, C. H. Back, and T. Jungwirth, *Rev. Mod. Phys.* **87**, 1213 (2015).
- [2] A. Hoffmann, *IEEE Trans. Magn.* **49**, 5172 (2013).
- [3] T. Seki, Y. Hasegawa, S. Mitani, S. Takahashi, H. Imamura, S. Maekawa, J. Nitta, and K. Takanashi, *Nat. Mater.* **7**, 125 (2008).
- [4] O. Mosendz, J. E. Pearson, F. Y. Fradin, G. E.W. Bauer, S. D. Bader, and A. Hoffmann, *Phys. Rev. Lett.* **104**, 046601 (2010).
- [5] L. Liu, C.-F. Pai, Y. Li, H.W. Tseng, D. C. Ralph, and R. A. Buhrman, *Science* **336**, 555 (2012).
- [6] E. Sagasta, Y. Omori, M. Isasa, M. Gradhand, L. E. Hueso, Y. Niimi, Y. C. Otani, and F. Casanova, *Phys. Rev. B* **94**, 060412(R) (2016).
- [7] C. Stamm, C. Murer, M. Berritta, J. Feng, M. Gabureac, P. M. Oppeneer, and P. Gambardella, *Phys. Rev. Lett.* **119**, 087203 (2017).
- [8] C. Chen, D. Tian, H. Zhou, D. Hou, and X. Jin, *Phys. Rev. Lett.* **122**, 016804 (2019).
- [9] T. Tanaka, H. Kontani, M. Naito, T. Naito, D. S. Hirashima, K. Yamada, and J. Inoue, *Phys. Rev. B* **77**, 165117 (2008).
- [10] L. Wang, R. J. H. Wesselink, Y. Liu, Z. Yuan, K. Xia, and P. J. Kelly, *Phys. Rev. Lett.* **116**, 196602 (2016).
- [11] Y. Sun, Y. Zhang, C. Felser, and B. Yan, *Phys. Rev. Lett.* **117**, 146403 (2016).
- [12] L. Berger, *Phys. Rev. B* **2**, 4559 (1970).
- [13] A. Crepieux and P. Bruno, *Phys. Rev. B* **64**, 014416 (2001).
- [14] S. K. Lyo and T. Holstein, *Phys. Rev. Lett.* **29**, 423 (1972).
- [15] H.-A. Engel, B. I. Halperin, and E. I. Rashba, *Phys. Rev. Lett.* **95**, 166605 (2005).
- [16] W. K. Tse and S. Das Sarma, *Phys. Rev. Lett.* **96**, 056601 (2006).
- [17] E. M. Hankiewicz and G. Vignale, *Phys. Rev. B* **73**, 115339 (2006).
- [18] W. Kohn and J. M. Luttinger, *Phys. Rev.* **108**, 590 (1957); J. M. Luttinger, *Phys. Rev.* **112**, 739 (1958).
- [19] N. A. Sinitsyn, *J. Phys.: Condens. Matter* **20**, 023201 (2008).
- [20] N. A. Sinitsyn, Q. Niu, and A. H. MacDonald, *Phys. Rev. B* **73**, 075318 (2006).
- [21] C. Xiao, J. Zhu, and B. Xiong, arXiv: 1811.06204
- [22] C. Xiao and Q. Niu, *Phys. Rev. B* **96**, 045428 (2017).
- [23] N. A. Sinitsyn, A. H. MacDonald, T. Jungwirth, V. K. Dugaev, and J. Sinova, *Phys. Rev. B* **75**, 045315 (2007).
- [24] C. Xiao, *Front. Phys.* **13**, 137202 (2018).
- [25] J. M. Ziman, *Principles of the Theory of Solids* (Cambridge University Press, Cambridge, 1972).
- [26] Y. Liu, Z. Yuan, R. J. H. Wesselink, A. A. Starikov, M. van Schilfgaarde, and P. J. Kelly, *Phys. Rev. B* **91**, 220405(R) (2015).
- [27] O. V. Dimitrova, *Phys. Rev. B* **71**, 245327 (2005).
- [28] S. Y. Liu and X. L. Lei, *Phys. Rev. B* **72**, 155314 (2005).
- [29] J. Schliemann and D. Loss, *Phys. Rev. B* **71**, 085308 (2005).
- [30] B. A. Bernevig and S. C. Zhang, *Phys. Rev. Lett.* **95**, 016801 (2005).
- [31] R. Moriya, K. Sawano, Y. Hoshi, S. Masubuchi, Y. Shiraki, A. Wild, C. Neumann, G. Abstreiter, D. Bougeard, T. Koga, and T. Machida, *Phys. Rev. Lett.* **113**, 086601 (2014).
- [32] H. Liu, E. Marcellina, A. R. Hamilton, and D. Culcer, *Phys. Rev. Lett.* **121**, 087701 (2018).
- [33] For our purpose of showing the T -dependence of the SHC induced by el-ph scattering, the results for $j_{\text{SH}}^{\text{sj}}$ and $j_{\text{SH}}^{\text{ad}}$ are sufficient. For completeness, we present in Ref. [34] the other spin Hall contribution of order $(W_{\mathbf{k}\mathbf{k}'})^0$ from the antisymmetric part of the third-Born-order scattering rate. This contribution also vanishes when $j_l^0 = 0$.
- [34] See Supplemental Material for the transport formalism for the SHCs of order $(W_{\mathbf{k}\mathbf{k}'})^0$ and calculation details of the SHC in the k -cubic Rashba model.
- [35] H. L. Stormer, L. N. Pfeiffer, K. W. Baldwin, and K. W. West, *Phys. Rev. B* **41**, 1278(R) (1990).
- [36] D. K. Efetov and P. Kim, *Phys. Rev. Lett.* **105**, 256805 (2010).
- [37] E. H. Hwang and S. Das Sarma, *Phys. Rev. B* **77**, 115449 (2008).
- [38] A. A. Abrikosov, L. P. Gor'kov, and I. E. Dzyaloshinskii, *Quantum Field Theoretical Methods in Statistical Physics* (Pergamon Press, New York, 1965); J. Rammer

- and H. Smith, *Rev. Mod. Phys.* **58**, 323 (1986).
- [39] S. Murakami, *Phys. Rev. B* **69**, 241202(R) (2004).
- [40] J. M. Ziman, *Electrons and Phonons* (Clarendon, Oxford, 1960).
- [41] Anton A. Starikov, Yi Liu, Zhe Yuan and Paul J. Kelly, *Phys. Rev. B* **97**, 214415 (2018).
- [42] G. K. White and S. B. Woods, *Phil. Trans. Roy. Soc. (London)* **A251**, 273 (1958).
- [43] R. H. Freeman, F. J. Blatt, and J. Bass, *Phys. Kondens. Materie* **9**, 271 (1969).